INTERNATIONAL JOURNAL OF PRECISION ENGINEERING AND MANUFACTURING Vol. 15, No. 2, pp. 339-343 FEBRUARY 2014 / 339
DOI: 10.1007/s12541-014-0343-8

Analysis on the Photovoltaic Property of Si Quantum Dot-Sensitized Solar Cells

Hyunwoong Seo[1,2,#], Daiki Ichida[1], Giichiro Uchida[3], Kunihiro Kamataki[1], Naho Itagaki[1], Kazunori Koga[1], and Masaharu Shiratani[1,2]

1 Graduate School of Information Science and Electrical Engineering, Kyushu University, 744 Motooka, Nishi-ku, Fukuoka, Japan, 819-0395
2 Center of Plasma Nano-interface Engineering, Kyushu University, 744 Motooka, Nishi-ku, Fukuoka, Japan, 819-0395
3 Joining and Welding Research Institute, Osaka University, 11-1 Mihogaoka, Ibaraki, Japan, 567-0047
Corresponding Author / E-mail: woong_1980@hotmail.com, TEL: +81-92-802-3723, FAX: +81-92-802-3723

KEYWORDS: Si quantum dot, Quantum dot-sensitized solar cell, Si-TiO_2 film, Multi-hollow plasma discharge CVD

This work first introduced Si quantum dots (QDs) for QD-sensitized solar cells (QDSCs). However, the particle size of Si QDs, which had visible light absorption, was relatively large. The paint-type Si QDSC was proposed in this work because Si QDs could not penetrate into nano-porous TiO_2 network. Si QDs were synthesized by multi-hollow plasma discharge CVD and mixed with TiO_2 paste. For better performance, thickness of Si-TiO_2 layer was varied by coating times and Si-TiO_2 films were optically and electrically analyzed. As a result, 6 times screen printed Si-TiO_2 film had the best performance with the smallest internal impedance and the highest photon to current efficiency.

Manuscript received: October 4, 2013 / Accepted: December 6, 2013

1. Introduction

Photochemical solar cells have attracted considerable attention with its simple process and low cost in the research field of photovoltaics.[1-6] They generally consist of sensitized TiO_2 electrode, catalytic counter electrode, and redox electrolyte. Various sensitizers such as dyes, organics, and quantum dots (QDs) were applied so far. Especially, QDs are expected to surpass Schockley and Queisser limit.[7] Their multiple exciton generation enhanced theoretical efficiency of photochemical solar cell from 33 to 44%.[8] In a previous work, we first introduced Si QD as an alternative to conventional QD materials such as CdS, CdSe, PbS, and PbSe due to their toxicity and scarcity.[9-12] Si is one of good QD materials and its quantum characteristics were already proved.[13,14] In addition, Si QD has high stability against light soaking as compared with a-Si:H films and a high optical absorption coefficient due to its quantum size effect as compared with ìc-Si films. Initial Si QD-sensitized solar cell (QDSC) had extremely low performance because of large particle size of Si.[15] In the sensitizing process, Si QDs could not penetrate into nano-porous TiO_2 network. However, it was difficult to reduce particle size because small Si particles absorbed UV light not visible light. Therefore, this work proposed paint-type solar cell using mixed TiO_2 and Si QDs. The heat-durability of Si QD is suitable for the paint-type solar cell while Ru dye widely used for photochemical solar cell has heat deterioration at even low temperature. The photovoltaic property of Si QDSC according to thickness of the photo electrode was optically and electrically analyzed in this work. The thickness was varied by the number of coating times. In order to characterize them, the photovoltaic performance, morphological property, incident photon to current conversion efficiency (IPCE), and internal electrochemical impedance were examined.

2. Experimental

2.1 Synthesis of Si QDs

Si QDs were synthesized by multi-hollow discharge plasma chemical vapor deposition (CVD).[15-19] Schematic diagram of the fabrication process is shown in Fig. 1. Silane (SiH_4) and hydrogen (H_2) were injected from the bottom of the reactor. It flowed through hollows of electrodes and pumped out from the top of the reactor. SiH_4 was converted to high-ordered silane with SiH_2 and ionized. Then, crystalline Si was nucleated and grown in the discharge plasma region. Eq. (1) simplified this process.[20] AC 200 W power with 60 MHz was applied to the electrode for the discharge at the room temperature.

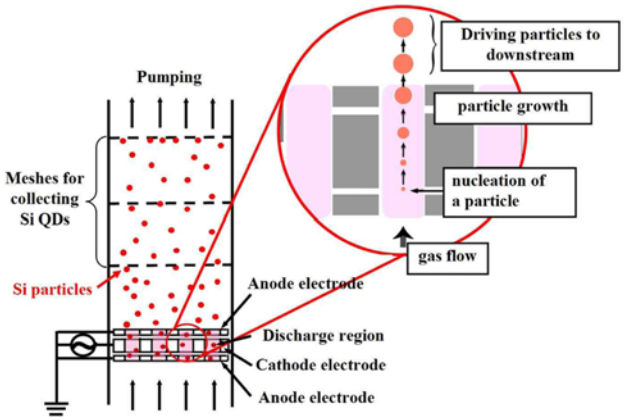

Fig. 1 Schematic of multi-hollow discharge plasma CVD

Generated Si QDs were transported to the downstream region with gas flow and captured by stainless-steel meshes. Si QDs were obtained by sonicating these meshes. This method is different from general Si QD fabrication based on etching or growing from Si substrate.[21-25] The crystallinity and particle size of Si QDs were controlled by the gas ratio of SiH_4 and H_2, and working pressure. Si QDs were structurally characterized by a transmission electron microscopy (TEM, JEM-2010, JEOL).

$$\begin{aligned} &SiH_4 + e^- \rightarrow SiH_2 + H_2 + e^- \\ &SiH_4 + SiH_2 \rightarrow Si_2H_6 \\ &Si_2H_6 + SiH_2 \rightarrow Si_3H_8 \\ &Si_3H_8 + SiH_2 \rightarrow Si_4H_{10} \\ &Si_4H_{10} + e^- \rightarrow Si_4H_{10}^-(grow) \end{aligned} \quad (1)$$

2.2 Fabrication of Si QDSCs

Si QDSCs were fabricated as follows. FTO substrates (15 Ω/sq., Nippon Sheet Glass) were used as the transparent conductive oxide (TCO) to make the photo and counter electrodes. The substrates were sequentially cleaned by sonicating in ethanol and dried using a stream of nitrogen. Si QDs were mixed with TiO_2 paste (HT-SP, Solaronix) by ballmill (PM100, Retsch). Si amount was 20 wt% vs TiO_2 and the paste was uniformly mixed with 400 rpm for 10 min. TiO_2-Si QD paste was coated on the cleaned FTO substrate by the screen print method. FTO/TiO_2-Si QD electrodes were sintered at 200°C for 30 min. Sintering process was conducted under vacuum for the prevention of Si QD oxidization. Au counter electrode with a thickness of about 100 nm was deposited by DC sputter (JEC-550, JEOL) at a power of 1.5 kVA and a working pressure of 2 Pa. After that, the photo and counter electrodes were sealed using a thermoplastic sealant (Meltonix 1170-25, Solaronix). The sealed Si QDSCs were completed by injecting a redox electrolyte through a pre-drilled hole into the counter electrode. The redox electrolyte consisted of 1 M Na_2S, 2 M S and 0.4 M KCl in water and methanol mixed solution at a volume ratio of 3:7.

2.3 Characterization

Before their characterization, the completed cells were stored in the dark under open-circuit conditions for 24 h to allow the electrolyte to penetrate into the pores. The photovoltaic performance was measured under 1 sun (air mass 1.5, 100 mW/cm^2) by a source meter (Model-2400, Keithley). IPCE (SM-250-P1, Bunkoukeiki) was measured from 250 to 900 nm. During their irradiance and characterization, the cells were covered with a black mask fitting the active area. The irradiated cell area was 0.20 cm^2. I-V characteristic curve and Eq. (2) were used to calculate the short-circuit current (I_{SC}) and density (J_{SC}), open-circuit voltage (V_{OC}), fill factor (FF) and the overall efficiency (η). The electrochemical analysis instrument (SP-150, Biologic SAS) was used to analyze the electrochemical impedance spectroscopy (EIS). EIS spectra were measured in the frequency range from 10 mHz to 1 MHz at room temperature. The applied bias voltage and AC amplitude were set at V_{OC} of QDSC and 10mV, respectively. The electrical impedances were characterized using the Nyquist diagram.

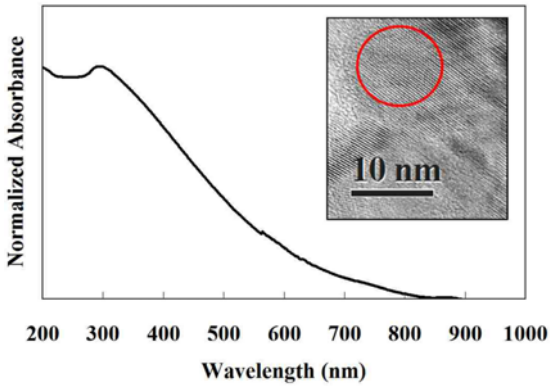

Fig. 2 Optical property and TEM image of 9 nm sized Si QD

$$\eta = \frac{Pmax}{Pin} \times 100 = \frac{FF \cdot Voc \cdot Jsc}{Pin} \times 100(\%) \quad (2)$$

3. Results and Discussion

The crystallinity and particle size of Si were controllable on the basis of our previous research.[18] Si was turned from amorphous to crystalline with the increase H_2 gas rate. Crystalline Si particles were obtained under SiH_4 and H_2 gas stream of 2 and 448 sccm. With this gas ratio, the working pressure was varied from 2 to 6 Torr. The particle size of crystalline Si was larger with the increase of pressure. Under high pressure, more particles were injected to the reactor and mean free path was shortened. Then, Si particles stayed in the discharge region for a longer time. That is, it was enough to react like Eq. (1) and generate more high-ordered silane as the seed of Si nano-particles. Accordingly, large Si particles were fabricated under high working pressure. Si particle size was changed from 5 to 17 nm. In this work, 9 nm sized Si QDs with visible light absorption were used under working pressure of 5 Torr as shown in Fig. 2.

Generated Si QDs were applied to Si QDSC. Si QDSCs were varied by screen printing (SP) times. Fig. 3 shows Si-TiO_2 film thickness according to SP times. Fig. 4 shows (a) their I-V characteristic curves and (b) each photovoltaic parameter. V_{OC} was increased with thickness of Si-TiO_2 film thickness but it was turned to decrease from 8 SP times. V_{OC} is determined by the difference between Fermi level of TiO_2 and redox potential. Dark photovoltaic property shows V_{OC} change because

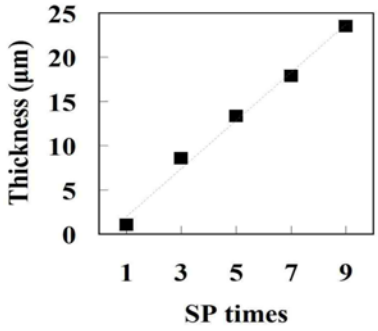

Fig. 3 Thickness of Si-TiO_2 film according to screen printing times

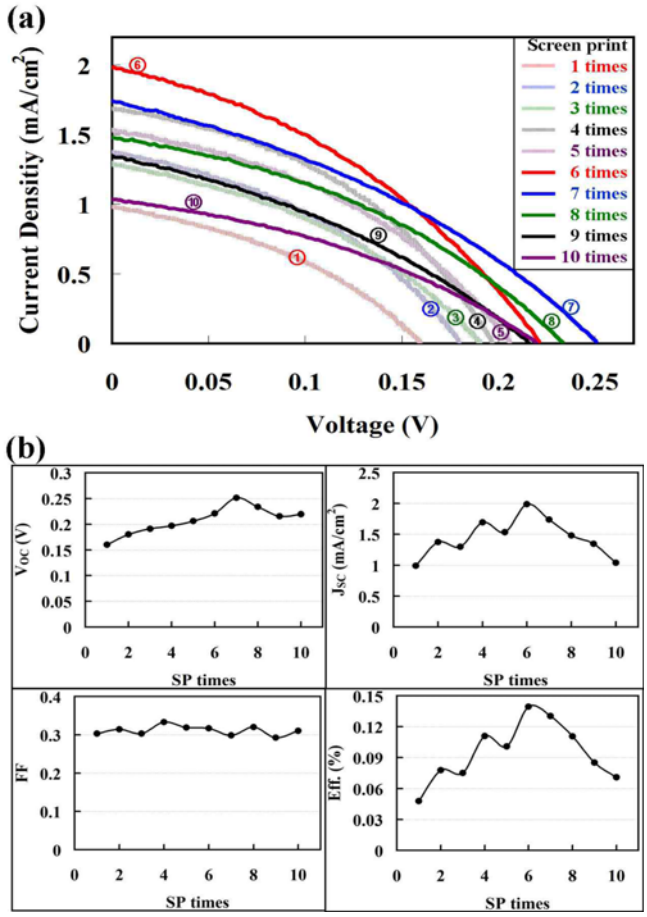

Fig. 4 (a) I-V characteristic curves of Si QDSCs according to screen printing times and (b) arranged photovoltaic parameters

dark current is tardily increased with higher V_{OC}.

Fig. 5 shows dark I-V characteristic curves of Si QDSCs according to SP times. Inset was helpful to compare their dark characteristics. At same dark current point (-3 mA/cm^2), voltage was increased with SP times. It was turned to decrease from 8 SP times. It accorded with a result of V_{OC} change. J_{SC} was also increased with Si-TiO_2 film and it was turned to decrease from 7 SP times. Thicker Si-TiO_2 film is able to generate more electrons because the amount of Si QDs is increased with Si-TiO_2 film. However, the penetration of incident photon into Si-TiO_2 layer was limited at specific thickness because of opaque films. Therefore, the increase of photocurrent was also limited.

Fig. 6 shows IPCE of Si QDSCs according to screen printing times.

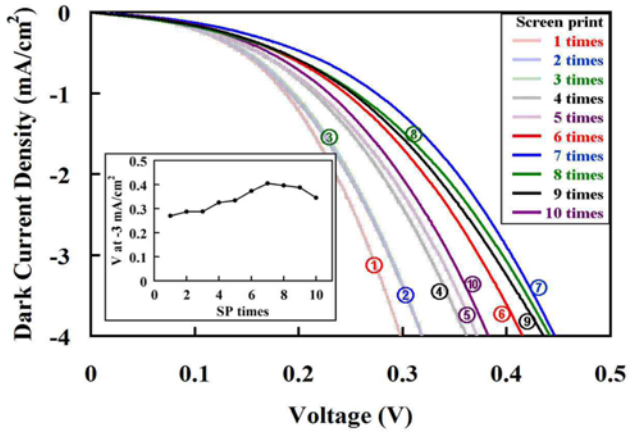

Fig. 5 Dark I-V characteristic curves of Si QDSCs according to screen printing times

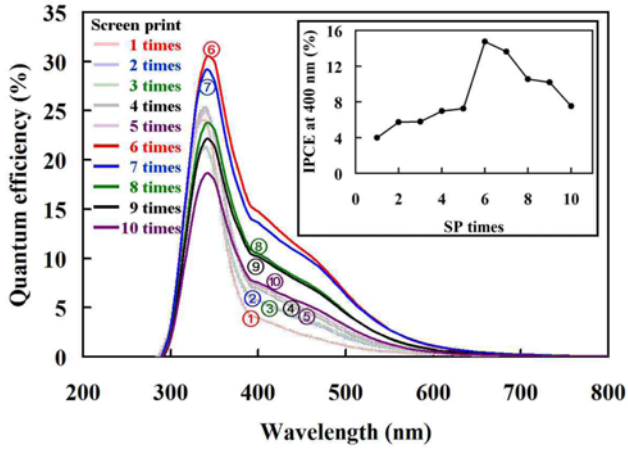

Fig. 6 IPCE of Si QDSCs according to screen printing times

Si-TiO_2 films absorbed the incident light from 300 to 700 nm wavelength range. The peak at 350 nm was mainly contributed by TiO_2 because its absorbance range was between 300 and 400 nm. Therefore, the absorbance in the wavelength range from 400 to 700 nm was important to analyze the photo-generation of Si QDs. Inset shows their IPCE values at 400 nm. 6 times screen printed Si-TiO_2 film had the highest peak. As mentioned above, increased Si QDs generated more electrons with thicker layer up to 6 SP times. However, exceeded Si QDs could not generate electrons in Si-TiO_2 films screen printed over 7 times and they disturbed charge transfer. The charge transfer was compared by internal impedance analysis.

Fig. 7(a) shows EIS spectra of Si QDSCs according to SP times. In general Nyquist diagram for EIS analysis, three impedances (Z_H, Z_M, Z_L) are observed in the high (over 1 kHz), middle (1 Hz to 1 kHz), and low (below 1 Hz) frequency range, and the resistance by the sheet resistance of TCO is detected over 1 MHz. These impedances are attributed to the charge transportation at the counter electrode, the electron transfer at the TiO_2/Si QD/electrolyte interfaces, and the charge transportation by ions in the electrolyte in the high, middle and low frequency range, respectively.[26-31] The total impedance is criterion of electron generation because total resistance in EIS diagram was inversely proportional to the overall performance. The change of total resistance and middle

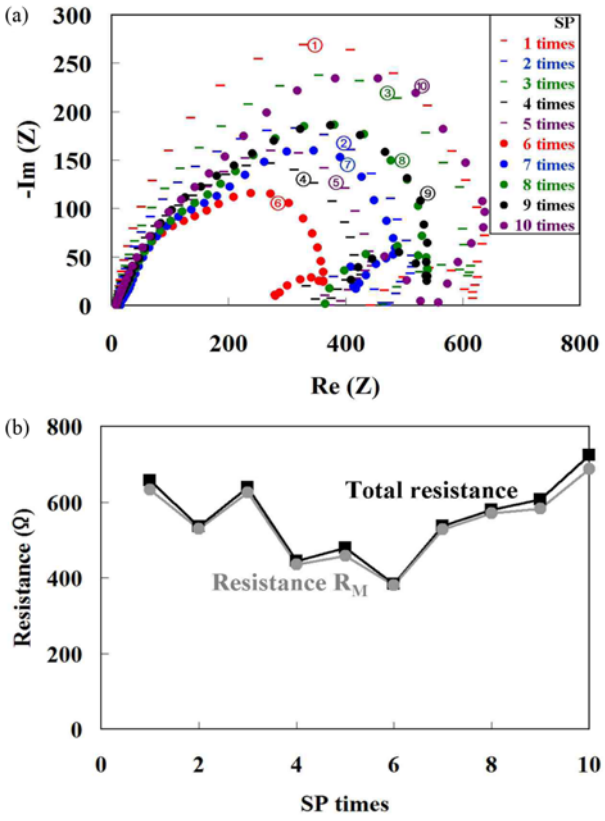

Fig. 7 (a) EIS spectra of Si QDSCs according to screen printing times and (b) the change of total resistance and R_M

frequency range resistance (R_M) were shown in Fig. 7(b). Internal impedance was decreased with thickness of Si-TiO_2 film. However, it was turned to increase from Si-TiO_2 film of 7 SP times. That is, the disturbance of charge transfer by exceeded Si QDs contributed to increase internal impedance because the electron transfer at the TiO_2/Si/electrolyte (R_M) was dominant in EIS analysis. Furthermore, Si-TiO_2 films screen printed over 8 times were partially peeled off due to too thick layer and repeated drying. Therefore, the photocurrent was limited by thickness of Si-TiO_2 film and 6 SP times had the highest photocurrent consequently. The overall performance was dominantly determined by the photocurrent although V_{OC} change was slightly different. Every FF was around 0.31. As a result, the best performance with 6 SP times was defined by 0.22 V of V_{OC}, 1.99 mA/cm^2 of J_{SC}, 0.32 of FF, and 0.14 % of efficiency.

4. Conclusions

In the research of photochemical solar cell, QDs are expected to enhance the performance with their multiple exciton generation characteristics. This work introduced Si QD as one of alternatives to conventional QD materials. Si QDs were fabricated by multi-hollow plasma discharge CVD and applied to Si QDSC. TiO_2 paste was mixed with Si QDs for uniform dispersion because of large Si particle size. The heat-durability of Si QD enabled to realize the fabrication of paint-type QDSC. For better performance of Si QDSCs, they were analyzed by Si-TiO_2 film thickness. The change of V_{OC} and J_{SC} was verified by dark current and IPCE, respectively. The disturbance of charge transfer by exceeded Si QDs was electrically analyzed by EIS. As a result, 6 times screen printed Si-TiO_2 film had the best performance although thicker Si-TiO_2 films had more Si QDs.

ACKNOWLEDGEMENT

This work was supported by MEXT KAKENHI Grant Number 211 10005.

REFERENCES

1. O'Regan, B. and Grätzel, M., "A Low-Cost, High-Efficiency Solar Cell based on Dye-Sensitized Colloidal TiO2 Films" Nature, Vol. 353, pp. 737-740, 1991.
2. O'Regan, B., Grätzel, M., and Fitzmaurice, D., "Optical Electrochemistry I: Steady-State Spectroscopy of Conduction-Band Electrons in a Metal Oxide Semiconductor Electrode," Chemical Physics Letters, Vol. 183, No. 1–2, pp. 89-93, 1991.
3. Yella, A., Lee, H. W., Tsao, H. N., Yi, C., Chandiran, A. K., and et al., "Porphyrin-Sensitized Solar Cells with Cobalt (II/III) - Based Redox Electrolyte Exceed 12 Percent Efficiency," Science, Vol. 334, No. 6056, pp. 629-634, 2011.
4. Kim, M. S., Chun, D. M., Choi, J. O., Lee, J. C., Kim, K. S., and et al., "Room Temperature Deposition of TiO2 using Nano Particle Deposition System (NPDS): Application to Dye-Sensitized Solar Cell (DSSC)," Int. J. Precis. Eng. Manuf., Vol. 12, No. 4, pp. 749-752, 2011.
5. Nagata, M., Baldwin, E., Kim, S., and Taya, M., "Design of Dye-Sensitized Solar Cells Integrated in Composite Panel Subjected to Bending," Journal of Composite Materials, Vol. 47, No. 1, pp. 27-32, 2013.
6. Seo, H., Son, M. K., Shin, I., Kim, J. K., Lee, K. J., and et al., "Faster Dye-Adsorption of Dye-Sensitized Solar Cells by Applying an Electric Field," Electrochimica Acta, Vol. 55, No. 13, pp. 4120-4123, 2010.
7. Shockley, W. and Queisser, H. J., "Detailed Balance Limit of Efficiency of p-n Junction Solar Cells," Journal of Applied Physics, Vol. 32, No. 3, pp. 510-519, 1961.
8. Murphy, J. E., Beard, M. C., Norman, A. G., Ahrenkiel, S. P., Johnson, J. C., and et al., "PbTe Colloidal Nanocrystals: Synthesis, Characterization, and Multiple Exciton Generation," Journal of the American Chemical Society, Vol. 128, No. 10, pp. 3241-3247, 2006.
9. Robel, I., Subramanian, V., Kuno, M., and Kamat, P. V., "Quantum Dot Solar Cells. Harvesting Light Energy with CdSe Nanocrystals Molecularly Linked to Mesoscopic TiO_2 Films," Journal of the American Chemical Society, Vol. 128, No. 7, pp. 2385-2393, 2006.
10. Blackburn, J. L., Selmarten, D. C., Ellingson, R. J., Jones, M., Micic, O., and Nozik, A. J., "Electron and Hole Transfer from

Indium Phosphide Quantum Dots," Journal of Physical Chemistry B, Vol. 109, No. 7, pp. 2625-2631, 2005.

11. Ju, T., Graham, R. L., Zhai, G., Rodriguez, Y. W., Breeze, A J., and et al., "High Efficiency Mesoporous Titanium Oxide PbS Quantum Dot Solar Cells at Low Temperature," Applied Physics Letters, Vol. 97, No. 4, pp. 043106, 2010.
12. Chen, Y., Maniruzzaman, M., and Kim, J., "Soft-Chemistry based Fabrication of Gallium Nitride Nanoparticles," Int. J. Precis. Eng. Manuf., Vol. 12, No. 3, pp. 573-576, 2011.
13. Beard, M. C., Knutsen, K. P., Yu, P., Luther, J. M., Song, Q., and et al., "Multiple Exciton Generation in Colloidal Silicon Nanocrystals," Nano Letters, Vol. 7, No. 8, pp. 2506-2512, 2007.
14. Wilcoxon, J. and Samara, G., "Tailorable, Visible Light Emission from Silicon Nanocrystals," Applied physics letters, Vol. 74, No. 21, pp. 3164-3166, 1999.
15. Seo, H., Wang, Y., Sato, M., Uchida, G., Kamataki, K., and et al., "Improvement of Si Adhesion and Reduction of Electron Recombination for Si Quantum Dot-Sensitized Solar Cells," Japanese Journal of Applied Physics, Vol. 52, No. 1, pp. 01AD05-01AD05-5, 2013.
16. Seo, H., Wang, Y., Uchida, G., Kamataki, K., Itagaki, N., and et al., "The Reduction of Charge Recombination and Performance Enhancement by the Surface Modification of Si Quantum Dot-Sensitized Solar Cell," Electrochimica Acta, Vol. 81, pp. 213-217, 2012.
17. Shiratani, M., Koga, K., Ando, S., Inoue, T., Watanabe, Y., and et al., "Single Step Method to Deposit Si Quantum Dot Films using H_2^+ SiH_4 VHF Discharges and Electron Mobility in a Si Quantum Dot Solar Cell," Surface and Coatings Technology, Vol. 201, No. 9-11, pp. 5468-5471, 2007.
18. Kakeya, T., Koga, K., Shiratani, M., Watanabe, Y., and Kondo, M., "Production of Crystalline Si Nano-Clusters using Pulsed H_2^+ SiH_4 VHF Discharges," Thin solid films, Vol. 506, No. pp. 288-291, 2006.
19. Seo, H., Wang, Y., Sato, M., Uchida, G., Koga, K., and et al., "The Improvement on the Performance of Quantum Dot-Sensitized Solar Cells with Functionalized Si," Thin Solid Films, Vol. 546, pp. 284-288, 2013.
20. Watanabe, Y., "Formation and Behaviour of Nano/Micro-Particles in Low Pressure Plasmas", Journal of Physics D: Applied Physics., Vol. 39, No. 19, pp. R329, 2006.
21. Nguyen, L. H., Le Thanh, V., Débarre, D., Yam, V., and Bouchier, D., "Selective Growth of Ge Quantum Dots on Chemically Prepared SiO_2/Si(001) Surfaces," Materials Science and Engineering: B, Vol. 101, No. 1-3, pp. 199-203, 2003.
22. Thanh, V. L., Ngo, T. T. T., Bui, H., Bouchier, D., Le, T. T. T., and Phan, K. H., "Selective Growth of SiGe Quantum Dots on Hydrogen-Passivated Si(100) Surfaces," Thin Solid Films, Vol. 428, No. 1-2, pp. 144-149, 2003.
23. Nakajima, A., Sugita, Y., Kawamura, K., Tomita, H. and Yokoyama, N., "Si Quantum Dot Formation with Low-Pressure Chemical Vapor Deposition", Japanese Journal of Applied Physics, Vol. 35, pp. 189-191, 1996.
24. Lee, S. C., Kim, C. K., Song, H. E., and Kim, Y. S., "Finite Element Analysis of Crystalline Silicon Solar Cell in Screen Printing Process by using Taguchi Method," Int. J. Precis. Eng. Manuf., Vol. 14, No. 4, pp. 635-642, 2013.
25. Hwang, D. S., Lee, C. H., Lee, J. O., Jeon, C. Y., Lim, Y. B., and et al., "Influences of Deposition Parameters on Micro-Crystalline Silicon Single Junction Cell Efficiency in Large-Area and High Rate Deposition," Int. J. Precis. Eng. Manuf., Vol. 13, No. 7, pp. 1113-1116, 2012.
26. Seo, H., Son, M. K., Park, S., Kim, H. J., and Shiratani, M., "The Blocking Effect of Charge Recombination by Sputtered and Acid-Treated ZnO Thin Film in Dye-Sensitized Solar Cells," Journal of Photochemistry and Photobiology A: Chemistry, Vol. 248, pp. 50-54, 2012.
27. Seo, H., Son, M. K., Kim, J. K., Choi, J., Choi, S., and et al., "Analysis of Current Loss from a Series-Parallel Combination of Dye-Sensitized Solar Cells using Electrochemical Impedance Spectroscopy," Photonics and Nanostructures - Fundamentals and Applications, Vol. 10, No. 4, pp. 568-574, 2012.
28. Han, L., Koide, N., Chiba, Y., Islam, A., and Mitate, T., "Modeling of an Equivalent Circuit for Dye-Sensitized Solar Cells: Improvement of Efficiency of Dye-Sensitized Solar Cells by Reducing Internal Resistance," Comptes Rendus Chimie, Vol. 9, No. 5-6, pp. 645-651, 2006.
29. Koide, N., Islam, A., Chiba, Y., and Han, L., "Improvement of Efficiency of Dye-Sensitized Solar Cells based on Analysis of Equivalent Circuit," Journal of Photochemistry and Photobiology A: Chemistry, Vol. 182, No. 3, pp. 296-305, 2006.
30. Han, L., Koide, N., Chiba, Y., Islam, A., Komiya, R., and et al., "Improvement of Efficiency of Dye-Sensitized Solar Cells by Reduction of Internal Resistance," Applied Physics Letters, Vol. 86, No. 21, pp. 213501-213503, 2005.
31. Seo, H., Son, M. K., Kim, H. J., and Shiratani, M., "Improvement on the Long-Term Stability of Dye-Sensitized Solar Module by Structural Alternation," Japanese Journal of Applied Physics, Vol. 51, No. 10, pp. 10NE21, 2012.